Extreme winds and the connection to reanalysis data

Xiaoli Guo Larsén, Jakob Mann and Hans E. Jøgensen

Risø National Laboratory, Wind Energy Department, Roskilde, Denmark

1. Introduction

The ultimate goal of this research is to build a worldwide extreme wind atlas. The need for the global extreme wind atlas is clear if one looks at the existing European Wind Load Code (Eurocode). When using the measurements of surface winds to evaluate the extreme winds, each country in Europe has established a procedure of their own, which leads to significant discontinuity of wind speeds at national borders, see e.g. Miller (2003). For instance, the 50-year wind is 24 ms^{-1} in southeast Denmark but 32 ms^{-1} in northern Germany. Taking into account that the forces (and in some cases also the price of the structure) increase as the square of the wind speed, this is a significant and unrealistic difference.

In this contribution we take the first steps in the construction of a global (or at least mid-latitude) extreme wind atlas based on the NCEP/NCAR reanalysis data. When estimating extreme winds, one needs long-term continuous time series, which are not always available. It is therefore a great advantage of using the reanalysis since it covers the whole globe and continuous for the entire record, and it covers more than 55 years. However, in addition, we also apply a unified procedure (as described by the statistical model in section 2) to long high quality time series of wind speed and direction from 132 stations in Europe, 1 from Greenland, and 3 from the Gulf of Suez. Both omni-directional and sector-wise distributions of the 50-year wind have been evaluated. The sector-wise distribution will provide important information about which direction the wind turbines to face.

2. The statistical model

The so-called "Annual Maximum Method" is applied to obtain the 50-year wind. The annual maximum winds are selected and sorted in ascending order (U_i^{max}) from n years' record. The distribution is then described by the double exponential, i.e. Gumbel distribution (Gumbel 1958):

$$F(U) = \exp(\exp(-\alpha(U - \beta)))\qquad(1)$$

where $F(U)$ is the cumulative probability; parameters α and β are estimated by

$$\alpha = \frac{\ln 2}{2b_1 - \overline{U^{max}}}, \quad \beta = \overline{U^{max}} - \frac{\gamma}{\alpha}\qquad(2)$$

where $\gamma\ (\approx 0.577216)$ is the Euler's constant, $\overline{U^{max}}$ is the mean maximum value and b_1 is calculated from U_i^{max}

$$b_1 = \frac{1}{n}\sum_{i=1}^{n}\frac{i-1}{n-1}U_i^{max}\qquad(3)$$

According to Abild (1994), this simple method of estimating α and β has been proven highly efficient for even small size samples.

From the cumulative probability for the recurrence interval $T = 1/(1-F(U_T))$, the T-year wind speed is obtained:

$$U_T = -\alpha^{-1}\ln\ln\frac{T}{T-1} + \beta\qquad(4)$$

3. 50-year wind from reanalysis data

The 50-year wind (U_{50}) is here defined as wind speed with a recurrence interval T=50 years, at 10 m high over a flat area with roughness length $z_0 = 0.05$ m. Frank (2001) has analyzed U_{50} based on surface wind records, wind speeds at 850 hPa as well as surface pressure over Denmark and found that using the surface pressure gives the best results and offers an opportunity for comparison with other data. We calculate U_{50} from pressure at the model surface (P_s) and temperature at 2 m (T_s) from the reanalysis data.

The reanalysis data are analysis of global weather observations with one modern numerical weather analysis and modelling system, which has being performed by the U.S. National Centers for Environment Prediction (NCEP) and the National Center for Atmospheric Research (NCAR) (Kalnay et al. 1996).

Pressure at the model surface is calculated on a Gaussian grid with longitudinal resolution 1.875° ($\Delta\lambda$) and a meridional resolution approximately 1.91° ($\Delta\phi$). It is a 6–hour forecast but influenced by observations. Data in use cover 55 years, from 1948 to 2002. Temperature at 2 m is available at the same grids.

In deriving U_{50} from the pressure we first need to extrapolate the surface pressure to one height, here the sea level. This is done by applying

$$P_0 = P_s \exp\left(\frac{gh}{RT_m}\right),\qquad(5)$$

where P_0 is the pressure at the sea level, g is the gravitational acceleration, h is the elevation and T_m is the mean temperature of T_s and T_0; T_0 the temperature at sea level, extrapolated from T_s at a lapse rate 6.5°C/1km. The geostrophic wind at sea level is then calculated with the pressure gradients,

$$u_g = -\frac{1}{f\rho}\frac{\Delta P}{2r\Delta\phi}, \quad v_g = \frac{1}{f\rho}\frac{\Delta P}{2r\Delta\lambda\cos\phi},\qquad(6)$$

where f is the Coriolis parameter, r is the earth radius, ϕ is the latitude, λ is the longitude, and ρ is the density. ΔP is across $2\Delta\phi$ and $2\Delta\lambda$. Thus U_{50} at

grid point [i,j] is calculated from 5 grid points ([i-1,j], [i+1,j], [i,j-1], [i,j+1], [i,j]). Assuming the geostrophic wind at sea level (u_g, v_g) be the wind above the boundary layer G, so that $G = \sqrt{u_g^2 + v_g^2}$.

By using the Annual Maximum Method, the 50-year omni-directional as well as sector-wise (in 12 sectors) geostrophic winds are obtained. The surface winds U_{50} at 10 m over z_0=0.05 m can then be converted from the 50-year geostrophic wind by solving the geostrophic drag law

$$G = \frac{u_*}{\kappa} \sqrt{\left(\ln \frac{u_*}{f z_0} - A \right)^2 + B^2} \qquad (7)$$

for u_*, where κ=0.4 is the von Karman constant, and A and B are dimensionless parameters. Here A=1.8, B=4.5, as used in Mortensen et al. (1993) are used. With u_*, the logarithmic wind law gives wind speed at 10m:

$$u_{10} = \frac{u_*}{\kappa} \ln \frac{10m}{z_0} \qquad (8)$$

4. Results

The 50-year wind U_{50} has been calculated for the northern hemisphere. Due to the method used, only the regions apart from the equator are valid. In Figure 1, contours of U_{50} are given for the region north of 15°N. The hotspots in the Pacific and Atlantic Oceans are clear. However there also show up unexpected hotspots over the Tibet Plateau, the Rocky Mountains as well as southern part of Greenland, which will be discussed in the next section.

A closer look at the region over northwest Europe, over 13°W – 13°E and latitude 45°N – 60°N, see Figure 2. U_{50} from the reanalysis are presented as colour contours, and those bold integers are U_{50} obtained from measurements. The transitions of U_{50} values from measurements at the national borders are rather smooth, after the unified procedure being applied. The general pattern of the reanalysis U_{50} is that there is a decrease from northwest to southeast, from about 25 ms^{-1} to about 17 ms^{-1}. It's worth mentioning that Figure 2 presents an area the same as that presented in Miller (2003), in which, every 6-hour weather maps of pressure have been used to evaluate the 50-year wind. Very similar to Miller's figure 5, Figure 2 also has a hotspot (24 ms^{-1}) in northern Ireland, and another extending across the North Sea into northern Germany (23 ms^{-1}). However one should be aware of that Miller's values have been corrected to 10 min values, while in Figure 2 these are still 6-hour predictions, with a time step of 20 min. Also, the reanalysis values are spatially averaged over grids. The crude temporal and spatial resolution will surely induce underestimation of the true extreme winds (see the detailed discussion in the next section), as also indicated by those bold numbers in this figure. The measurement data are

10 min averages saved every 3rd hour. Sector-wise distribution of U_{50} are calculated and compared with the reanalysis U_{50}. The agreement for the sector-wise distribution of U_{50} is very good in some countries, e.g. Belgium, Denmark, Germany, Ireland, the Netherlands, and some parts in France, Portugal, Spain and UK; mostly they show a strong dominant west wind. In some countries, like Greece and Italy, few sites give consistent measured and reanalysis sector-wise U_{50}.

Now we take an even closer look at the region over ~ 7°E – 13°E, ~ 50°N – 60°N, i.e. covering Denmark and northern Germany, see Figure 3. The notations are the same as those in Figure 2, additionally the values of reanalysis U_{50} are printed in thinner text. This figure of the reanalysis U_{50} is almost the same as that given in Frank (2001) with very few differences, which are induced by the following facts: we used data 1948-2002 while Frank used only 1953-1999; we use data at 00, 06, 12 and 18 UTC while Frank used data at 00 and 12 UTC; here mean temperature over the fictitious air column between the surface and sea level is used while in Frank T_s is used. The last brings negligible differences over Denmark, where the elevation is rather low. The general underestimation by the reanalysis is quite clear.

5. Discussions and conclusions

Not all the measurements are recorded as 10 min average. There may be several hours' temporal spacing between saved samples. The record is then obtained by so-called disjunct sampling. It may also happen that the wind speed is not averaged over 10 min, but over longer period of time. Both situations have a consequence that the true annual maximum, defined as the maximum 10 min average wind, is underestimated. The exact maximum of a strong wind event may fall between the measured 10 min averages. This is one of the uncertainties in estimating the extreme wind discussed by Mann et al. (1998). Continuous measurements from Sprogø (Denmark, 10-min averages 23 years record), Kap Molkte (Greenland, 1 hour averages over 10-min average values, 18 years record) and a couple of sites from the Gulf of Suez (10-min averages, 12 years record) have been used to explore the effects of different sampling strides and averaging times. The results are presented in Figure 4 and 5. A reduction of the annual maximum is about 7% at a disjunct stride of 3 hours, 10% at 6 hours and up to about 15% at 12 hours. And the reduction induced by the smoothing of averaging is even larger, about 10% when the averaging time is 3 hours and up to 20% when it is 12 hours. Thus, in order to compare with Miller's results, we will have to increase the reanalysis U_{50} by 10%, although strictly speaking, the reanalysis data are not 10 min averages sampled at every 6th hour. This accordingly leads to the fact that the reanalysis U_{50} are about 10% higher than

Miller's. This difference will be reduced to 3% if we change the values of parameters A and B in Equation (7) to those used by Miller (A=1.40 and B=5.79). For disjunct stride in Figure 4, the thick black curve is a theoretical approach in which the time series is treated as Gaussian Markov Chain. For averaging time in Figure 5, the theory is derived for Gaussian distributed time series. Exponential decay for the autocorrelation of the time series is applied, which, when measurements being examined, is a very good representation for the mid-latitude site Sprogø but not for those in the Gulf of Suez. However, for the omni-directional situation, the theories are quite good approximations, although the decrease rate of $U_{max}/U_{max,\ 10min}$ with disjunct stride and averaging time is expected to be related to the climate at that site. The decrease rate of $U_{max}/U_{max,\ 10min}$ with disjunct stride and averaging time for different sectors (12 sectors in total) has shown to be site-dependent. For Sprogø, although the west wind dominates, winds from other directions are not rare, so the curves are quite similar for 12 sectors. For the sites of the Gulf of Suez, about 75% of the time winds are from the north, which leads to $U_{max}/U_{max,10min}$ in other sectors than the north decreases very rapidly with disjunct stride as well as with averaging time.

Many uncertainties will be introduced during the calculation as described in section 2 and 3; this is clear when we go through the two sections. First, when applying the statistical model, long-term continuous records are required. Shorter time series are more likely to bring biased results. In this study, sites with measurement record over 7 years are selected; 7 years are far from an optimal data length.

Secondly, equation (5) is not supposed to work for complex terrains. Extrapolating the surface temperature to the sea level by using an assumed lapse rate over high elevations is not reliable, strictly speaking. This explains those unrealistic strong winds over the Tibet Plateau, Greenland and the Rocky Mountains. There have been many proposals in trying to solve this problem but this problem remains to be solved, see e.g. Mohr (2004) and Pauley (1998). For the reanalysis U_{50}, these erroneous values are present over regions where the elevation variation is significant.

One may expect uncertainties from the use of $G_{sea\ level}$=G. This has also been applied in Miller (2003), in which he examined his data and found a ratio of 0.46 between the geostrophic wind speed and wind at 10 m, which is consistent with the ratio between the wind speed at heights of 900 and 10 m predicted using the Harris and Deave (1981) wind speed profile for z_0=0.05 m. Here we obtained a ratio 0.45 for $G_{sea\ level}$ to wind at 10 m. $G_{sea\ level}$=G can be considered a reasonable assumption. No variation of G with height is accounted since no

horizontal temperature variation is taken into consideration. Nor is the vertical potential temperature variation considered since the atmosphere is in general neutral during extreme wind conditions. However, this is listed as one of the sources of bias in Mann et al. (1998).

The crude spatial resolution of the reanalysis will inevitably bring underestimation. Besides using 5-point, 4 and 3 neighbouring grid points have also been used to calculate U_{50}. It is found that the 4-point method gives an increase of 3% in U_{50} systematically. Another 3% increase is given when using the 3-point method.

Briefly, in spite of many assumptions applied, the 50-year wind U_{50} estimated from the sea level pressure gradient by using the reanalysis show to be quite reasonable over most part of the hemisphere; they also show to be good approximations when compared with measurements from Europe, both for omni-directional and sector-wise cases. Regions where other methods than the one applied in this study are needed are the tropical regions, high mountains and Plateaus.

Acknowledgement

References

Abild J., 1994: Application of the wind atlas method to extremes of wind climatology, Technical Report R-722(EN), Risø National Laboratory.

Bergström H., 1992: Distribution of extreme wind speed, Wind Energy Report 92:2, Department of Meteorology, Uppsala University, Sweden.

Frank H.P., 2001: Extreme winds over Denmark from the NCEP/NCAR reanalysis, Riso-R-1238 (EN), Risø National Laboratory.

Gumbel E.J., 1958: Statistics of extremes, Columbia University Press.

Harris R.I. and Deaves D.M., 1981: The structure of strong winds, in: Wind Engineering in the Eghties, Proceedings of the CIRIA conference held on 12-13 Nov. 1980, CIRIA, London, paper 4.

Kalnay E. and co-authers, 1996: The NCEP/NCAR 40-year reanalysis project, Bull. Am. Meteorol. Soc. 77, 437-471.

Mann J., Kristensen L. and Jensen N.O., 1998: Uncertainties of extreme winds, spectra and coherences, Bridge Aerodynamics, Larsen & Eddahl (eds), Balkema, Rotterdam, ISBN 9054109610.

Miller C., 2003: A once in 50-year wind speed map for Europe derived from mean sea level pressure measurements, J. Wind Eng. Ind. Aerodyn. 91, 1813-1826.

Mohr M., 2004: Problems with the mean-sea-level pressure field over the western United States, Monthly Weather Review, in press.

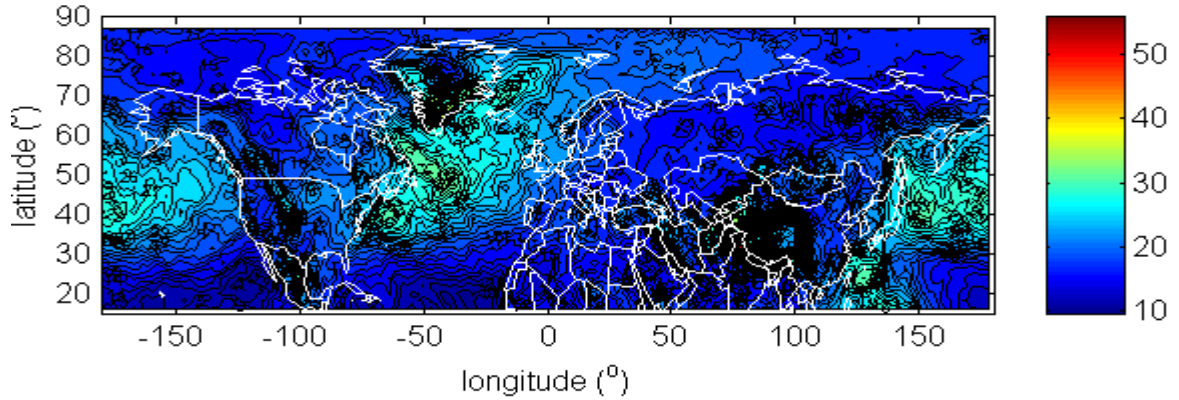Mortensen N.G., Landberg L., Troen I. and Petersen E.L., 1993: Wind atlas analysis and application program

(WA^{S}P). Vol 2: User's Guide. Technical Report I-666(EN), Risø National Laboratory.

Pauley P.M., 1998: An example of uncertainty in sea level pressure reduction, Wea. Forecasting, 13, 833-850.

Figure 1. U$_{50}$ from the reanalysis data in the northern hemisphere over longitude 180°W - 180°E, 15°N - 90°N, in contours marked with values; the white points show roughly the map over this region.
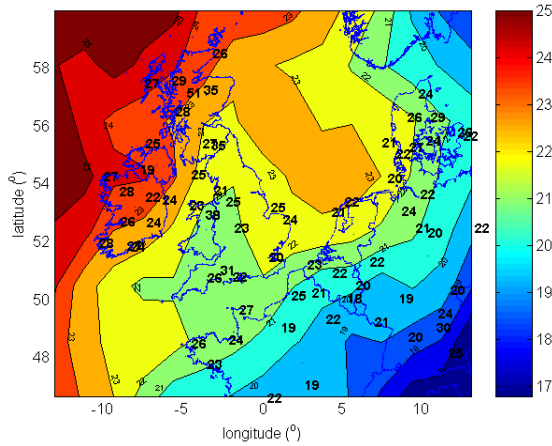
Figure 2. U$_{50}$ from the reanalysis data (colour contours marked with values) and from measurements (bold integers) over longitude 13°W – 13°E and latitude 45°N – 60°N
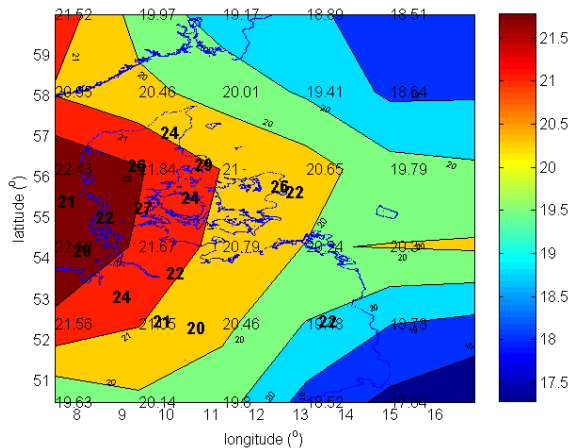

Figure 3. 50-year wind U$_{50}$ from the reanalysis data (colour contours and numbers at 30 grid points) and from measurements (bold integers) over Denmark and northern Germany
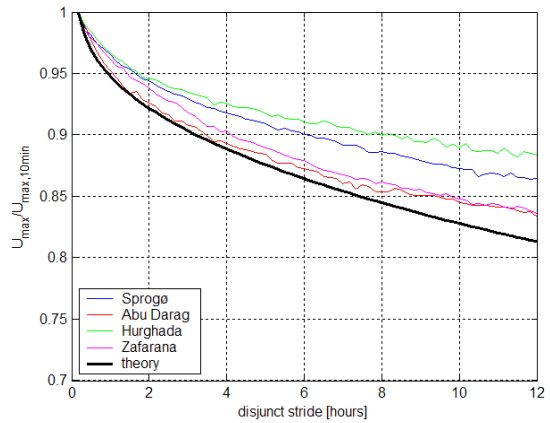

Figure 4. Annual wind maxima at different disjunct strides divided the 10-min annual wind maxima, as a function of disjunct stride, measurements as well as theory.
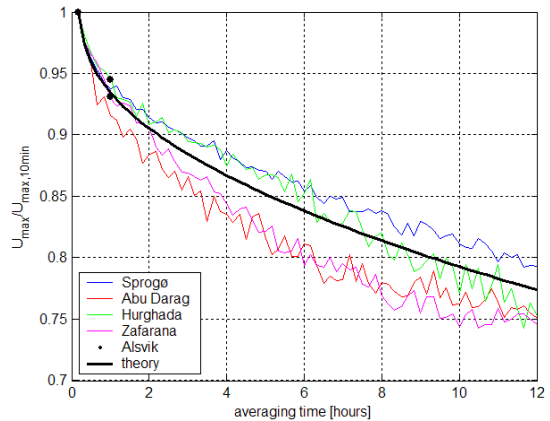

Figure 5. Annual wind maxima at averaging time divided the 10-min annual wind maxima, as a function of averaging time, measurements as well as theory. The dots (measurements from Alsvik, Sweden) are from Bergström (1992).

4